Home   Search   Collections   Journals   About   Contact us   My IOPscience

Shell model parameters for layered copper oxides

Shell model parameters for layered copper oxides

Valentin N Popov

Faculty of Physics, University of Sofia, 5 James Bourchier Boulevard, 1126 Sofia, Bulgaria

Abstract. The lattice dynamics of layered copper oxides is usually studied within the shell model using parameters obtained from calculations of simpler oxides. In this paper, this approach is complemented with a model treatment of the cation–oxygen short-range potential parameters. For two groups of ionic pairs, Ae^{2+}–O^{2-} and Re^{3+}–O^{2-} (where Ae is an alkaline earth element and Re is a rare earth element or yttrium), the estimated values of these parameters and various cation coordinations are applied in shell model calculations of Ca_2CuO_3, $(Pr, Sr)_2CuO_4$ (T, T', and T^* phases), $YBaCuFeO_5$, $YBa_2Fe_3O_8$ and $HgBa_2CuO_4$. The results of the calculations are found to be in reasonable agreement with the existing Raman and infrared data.

1. Introduction

The discovery in 1986 of high-T_c superconductivity in $La_{2-x}Sr_xCuO_4$ attracted considerable attention to the synthesis and investigation of layered copper oxides with perovskite-like structures. The origin of superconductivity in these materials remains unclear, despite the fact that numerous mechanisms, including electron–phonon interactions, have been proposed. Apart from the possible involvement of phonons in this phenomenon, a lattice-dynamical study of these compounds may be capable of expanding our knowledge of their physical characteristics.

The first lattice-dynamical investigations of layered copper oxides were made in 1986 as attempts to properly assign the features observed in the optical spectra of the newly discovered high-T_c superconductors. The calculations were initiated within the simple force-constant approach for La_2CuO_4 [1,2], $YBa_2Cu_3O_7$ [3,4] and $YBa_2Cu_3O_6$ [5,6]. The correspondence between the experimental and estimated zone-centre phonon frequencies was, however, rather vague. The reason for this was clearly the high ionicity of the copper oxides. A considerable improvement was achieved when the long-range Coulomb interactions of the ions in $YBa_2Cu_3O_7$ were included in a valence-force model [7]. The initial values of the numerous model parameters were adopted from related materials, but had to be additionally adjusted in order to reproduce the measured phonon frequencies.

The shell model, based on potential functions [8], gained enormous popularity among the phenomenological models. This model is extraordinarily simple, and uses a comparatively small number of model parameters. At the same time, it properly accounts for the predominant ionicity of the layered oxides, representing the interionic interactions as sums of long-range Coulomb parts and short-range (SR) ones, the latter being described by potentials in Born–Mayer form instead of by numerous meaningless force constants. Even so, many model parameters have to be introduced because the compounds of interest contain many atoms per unit cell. This difficulty is circumvented by the transfer of the necessary parameters from binary metal oxides and substances with perovskite structure, whose dynamical properties are well studied on the basis of fits to the experimental

dispersion curves, and optical, elastic and dielectric data. Following such an approach, the lattice dynamics of La_2CuO_4[9], $YBa_2Cu_3O_7$ [10], $Bi_2CaSr_2Cu_2O_8$ [11], various Tl-based compounds [12], $Y_{1-x}Pr_xBa_2Cu_3O_7$ [13] and, recently, $Nd_{2-x}Ce_xCuO_4$ [14] have been investigated. Apart from the overestimation of the frequencies of a few oxygen modes, in all cases the overall agreement with experimental data is good, verifying the efficiency of the potential function approach and justifying the transferability of the parameters to copper oxides.

Allan and co-workers [15, 16] implemented electron-gas potentials within the shell model in a study of the crystal and defect properties of the ternary cuprates Ae_2CuO_3 (where $Ae = Ca$, Sr and Ba) in a comparison with those of La_2CuO_4, in an attempt to understand why only the lanthanum cuprate leads to superconducting compounds. Calculations of their phonon modes using these potentials have not yet been published, however.

In this work we present transferable shell model parameters obtained on the basis of a model treatment of the interionic short-range interactions (section 2) and via fits to the experimental dispersion curves of CuO (section 3.1), neutron diffraction, optical, elastic and dielectric data on CaO, SrO and BaO (section 3.2), and to the Γ-point phonons of La_2CuO_4, $YBa_2Cu_3O_6$ and Nd_2CuO_4 (section 3.3). The results of the application of these parameters to calculations of the phonon modes of a number of layered copper oxides have already been, or soon will be, published elsewhere.

2. Model parameters

The shell model has been intensively used in studies of the phonon spectra of ionic compounds. In this model the interionic interactions are described by long-range Coulomb potentials and short-range potentials usually chosen to be of Born–Mayer form:

$$\phi(r) = a \exp(-br). \qquad (2.1)$$

Here a and b are parameters, and r is the distance between the ions. In order to account for the ionic polarizability, each ion is considered to consist of a charged massless shell surrounding a charged core, which are coupled together by a harmonic spring of spring constant k. The free ionic polarizability is expressed by

$$\alpha = \frac{(Ye)^2}{k} \qquad (2.2)$$

where Y is the dimensionless shell charge and e is the absolute value of the electron charge.

The ionic charges Z, the potential parameters (a and b) and the parameters describing the polarizability (Y and α) are usually obtained by least-squares fits to the measured phonon dispersion curves, and optical, dielectric and elastic quantities. The amount of experimental data on the layered copper oxides is insufficient for a determination of these parameters, and it is not always possible to transfer them from other better studied and simpler oxides. A shell model study can then only be carried out successfully on the basis of a systematic approach to the derivation of the model parameters, including the implementation of certain assumptions and model treatment [17]. Since this approach has proven its efficiency it is adopted here, and in all cases the five following assumptions are made.

(i) The ionic charges Z are equal to the nominal valency of the ions, reduced by a factor of 0.95 in order to account for charge screening. This is supported by the recent

theoretical evaluations of Z for CaO, SrO and BaO which yielded 1.88, 1.85 and 1.82, respectively [18].

(ii) The polarizability parameters Y and α are transferred from other compounds. If not stated otherwise, $\alpha_{O^{2-}}$ is fixed at 2.0 (in units of Å^3) (see, for example, [19]).

(iii) The SR cation–cation interactions are ignored.

(iv) The O^{2-}–O^{2-} SR potential of the Born–Mayer–Buckingham form

$$\phi(r) = a \exp(-br) - \frac{c}{r^6} \tag{2.3}$$

is essentially that obtained in [20].

(v) The cation–anion SR potential parameters are extrapolated from relationships that are discussed below.

A simple scheme for the derivation of SR parameters was proposed by Lewis and co-workers [17]. For structurally and chemically similar oxides, these authors accepted the same b, while the values of a were determined from the equilibrium conditions. The results of this assumption were found to be encouraging. The parameter b may, however, depend on the quantities of the physical problem and this dependence can be obtained using dimensional arguments. In fact, since b has the dimensions of L^{-1} (where L is length) and the equilibrium interionic separation R is the essential parameter for the cation–anion SR interaction with dimensions of length, then the following scaling law must be valid:

$$b = \frac{\beta}{R}. \tag{2.4}$$

Here β is a universal constant for the given group of ionic pairs, and is charge independent. This relation has a simple physical interpretation. Let us consider the crystal as being built out of hard spherical ions. The hardness, or the impossibility of adjacent ions to penetrate into one another, is a result of the abruptly increasing repulsive interaction between them as the interionic distance decreases. Since a short-range potential of the form (2.1) becomes essential for distances of the order of $1/b$, it may be assumed that, for different ionic pairs, b depends reciprocally on R. A relationship, analogous to (2.4), was also considered by other authors [21]. In the case of alkaline earth oxides the shell model result for β is very close to 7 (see table IV in [17]).

The R-dependence of a is difficult to determine on the basis of dimensional arguments alone. Let us consider the stability criterion [22], which states that for a crystal in equilibrium the components of the stress tensor vanish:

$$\sigma_{ii}^C + \sigma_{ii}^R = 0. \tag{2.5}$$

Here the Coulomb and SR parts are denoted by the indices 'C' and 'R', respectively, and $i = x, y, z$. For the case of alkaline earth oxides with NaCl structure

$$\sigma_{ii}^C = \alpha_M \frac{(Ze)^2}{R^2} \tag{2.6}$$

and

$$\sigma_{ii}^R = -6ab \exp(-bR) \tag{2.7}$$

where α_M is the Madelung constant (in the short-range interactions only the nearest cation–anion pairs are taken into account). The Coulomb part (2.6) is inversely proportional to the second power of R, while the SR one (2.7), in view of (2.4), depends reciprocally on R. Then, in order to maintain the validity of (2.5), when passing from one compound to another, a must obey the scaling law

$$a = \frac{\alpha^{(2)}}{R}. \tag{2.8}$$

The estimation of the universal constant $\alpha^{(2)}$ for Ae^{2+}–O^{2-} ionic pairs is discussed in section 3.2.

The relationship (2.8) is better fulfilled for ions with a nearly spherically symmetrical electron density, such as the alkaline earth ions. In the case of the 3d elements Mn, Fe, Co and Ni, perhaps because of their partially built d-electron layers, (2.8) no longer holds true. In fact, it appears that a is inversely proportional to the third power of R [17, 23]. Copper is less expected to follow (2.8), because CuO is monoclinic and the cations reside in the centres of distorted octahedra. Because of this, we derived the Cu–O potential via separate fits to the dispersion curves of cupric oxide (see section 3.1).

The layered copper oxides may also include rare earth elements and yttrium (denoted hereinafter as Re). The R-dependence of a for ionic pairs Re^{3+}–O^{2-} can be obtained using the equilibrium condition (2.5) for the special case of oxides Re_2O_3 with cubic bixbyte structure, in which each cation is surrounded by six nearly equidistant oxygen ions. The Coulomb and SR parts of the stress tensor components consist of several terms, but this fact does not qualitatively change the derivation. Taking into account (2.4), it follows from (2.5) that a must scale with interionic distance as given by (2.8), but with a different value of α:

$$a = \frac{\alpha^{(3)}}{R}. \tag{2.9}$$

The upper index '3' of $\alpha^{(3)}$ denotes that this constant refers to Re^{3+}–O^{2-} ionic pairs. The value of $\alpha^{(3)}$ is obtained in section 3.3.

In view of the implementation of the presented scheme to layered copper oxides, two more suppositions can be made. First, in the general case each cation is coordinated by non-equidistant oxygen ions and in (2.4), (2.8) and (2.9) one has to deal with different interionic separations. Instead of this, it is more convenient to use some average interionic distances. Secondly, the cations can have other than sixfold coordinations. In this case, the average interionic separation can be estimated as the sum of the average cation radius for the cation coordination number (N), equal to N, and the average O^{2-} radius, equal to 1.40 Å. Throughout this work the cation radii are taken from [24]. It must be pointed out that the equilibrium interionic separations change by up to 10% when the CN increases from VI to XII, and this leads to essential changes in the $\phi(r)$ curves. That is why, if the resulting lattice dynamics of a given copper oxide is stable, this may be considered as a test for the applicability of the proposed extrapolation scheme.

3. Results and discussion

3.1. Cupric oxide

The cupric oxide crystallizes in a monoclinic structure with space group $C2/c$ [25] (see figure 1). Each cation is square coordinated by four planar oxygen ions with nearly equal

Cu–O separations of about 1.96 Å. These ionic squares build ribbons running along the [110] and [1$\bar{1}$0] directions. The adjacent ribbons are coupled together by Cu–O bonds of length 2.78 Å. Thus, each copper ion is coordinated by a distorted octahedron of oxygen ions. Similar octahedra, elongated along one of the axes, exist in a number of layered copper oxides, which implies that the Cu–O interactions are of similar nature. This makes CuO a suitable compound for the study of these interactions and for obtaining transferable shell model parameters that can plausibly reproduce the vibrational modes of the cuprates.
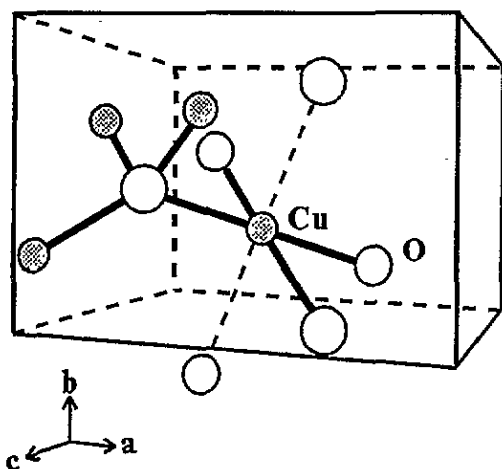

Figure 1. The unit cell of CuO (after [25]).

The lattice dynamics of CuO has already been studied using a 22-parameter rigid ion model and a 9-parameter shell model on the basis of Raman data [26] and phonon dispersion curves, measured by inelastic neutron scattering [27]. While with the former model a fair reproduction of the experimental curves was reached at the price of rather large third-nearest-neighbour Cu–Cu SR interactions, the shell model had to be improved by additionally introducing unphysical Cu–O transverse force constants. The attempts to describe the lattice dynamics of CuO with parameters, transferred from NiO [28], met with no success.

Here, the calculation of the phonon modes of CuO was carried out within the shell model and the assumptions listed in section 2. The 'intraplanar' (in-ribbon) and 'interplanar' (between adjacent ribbons) Cu–O SR interactions were supposed to be different, because they arise from the overlap of different electron orbitals. The parameters, obtained from fits to the experimental dispersion curves in the [100], [010] and [001] directions, are shown in table 1. The calculated dispersion curves, along with the measured frequencies, are displayed in figure 2.

Table 1. Shell model parameters for CuO. ($0_{\parallel}$ and $0_{\perp}$ denote 'intraplanar' and 'interplanar' Cu–O interactions, respectively.)

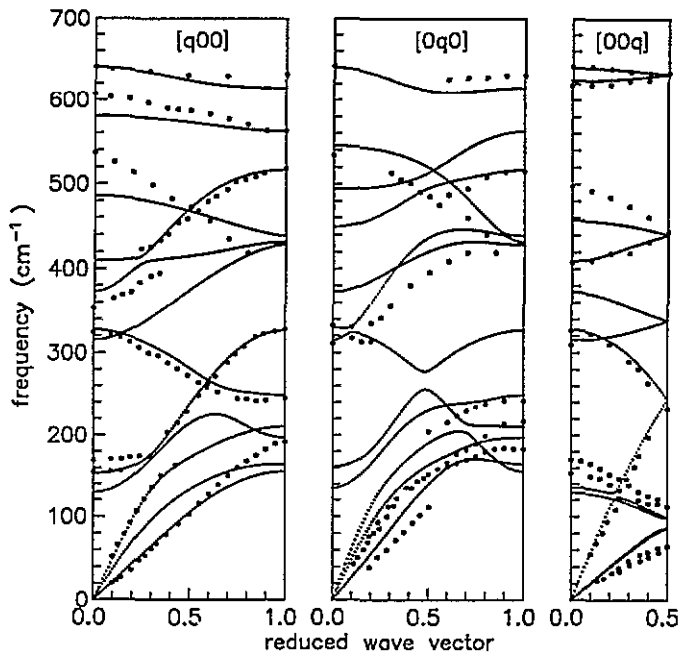| Ion	α (Å^3)	Y ($|e|$)	Ionic pair	a (eV)	b (Å^{-1})	c (eV Å^6)
Cu^{2+}	1.3	3.0	(Cu^{2+}–O^{2-})$_{\parallel}$	1600	3.553	0.0
			(Cu^{2+}–O^{2-})$_{\perp}$	550	2.518	0.0
O^{2-}	2.0	−3.0	O^{2-}–O^{2-}	22764	6.711	20.37

Figure 2. Phonon dispersion curves of CuO. The dotted curves are calculated with a shell model. The experimental points (circles) are taken from [27].

Table 2. Dielectric and elastic constants (in 10^{12} dyn cm^{-2}) for CaO, SrO and BaO: experiment and calculations.

Oxide	Dielectric constants		Elastic constants					
	Exp.	Calc.	Exp.				Calc.	
			C_{11}	C_{12}	C_{44}		C_{11}	$C_{12} = C_{44}$
CaO	3.33 [29]	3.30	2.26	0.62	0.81 [32]		2.08	0.86
SrO	3.46 [30]	3.45	1.73	0.45	0.56 [33]		1.52	0.65
BaO	3.92 [31]	3.88	1.12	0.36	0.34 [34]		1.10	0.49

Table 3. Shell model parameters for CaO, SrO and BaO.

Ion	α (Å^3)	Y ($|e|$)	Ionic pair	a (eV)	b (Å^{-1})	c (eV Å^6)
Ca^{2+}	1.5	4.5	Ca^{2+}–O^{2-}	1021	2.917	0.0
Sr^{2+}	2.5	4.5	Sr^{2+}–O^{2-}	950	2.713	0.0
Ba^{2+}	3.6	5.6	Ba^{2+}–O^{2-}	891	2.545	0.0
O^{2-}	2.0	−3.0	O^{2-}–O^{2-}	22764	6.711	20.37

3.2. Alkaline earth oxides

The alkaline earth oxides CaO, SrO and BaO crystallize in the NaCl structure. A lot of optical, dielectric and elastic data on these oxides were gathered (see table 2). In addition, neutron diffraction measurements were carried out in the symmetry directions in the Brillouin zone (figure 3). The lattice dynamics of these oxides has been intensively studied in the last three decades [39]. In this paper, however, it is considered on the basis of the assumptions
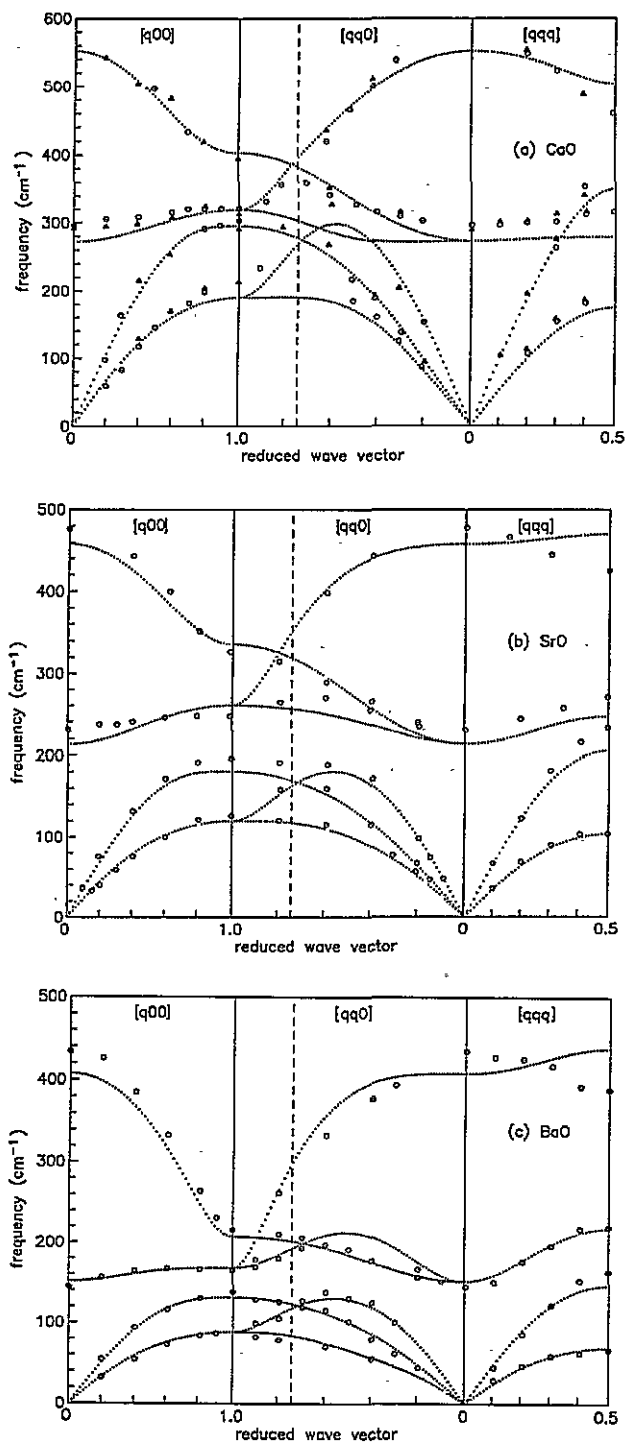
Figure 3. Phonon dispersion curves of alkaline earth oxides. The dotted curves are calculated with a shell model. The experimental points are taken from: (a) CaO [35] (circles) and [36] (triangles), (b) SrO [37] (circles) and (c) BaO [38] (circles).

listed in section 2. The input cation polarizabilities, taken from [40], were slightly varied in the fitting procedure. The cation–anion SR potential parameters were supposed to follow common scaling laws (2.4) and (2.8). The universal parameter β was fixed at 7.0 [17], while $\alpha^{(2)}$ was to be determined. In the SR interactions only the nearest neighbours were accounted for.

Table 4. Short-range parameters for alkaline earth–oxygen ionic pairs for N-fold cation coordination ($\alpha^{(2)} = 2450\,\text{eV Å}$, $\beta = 7.00$).

Ion	Parameter	Coordination number						
		VI	VII	VIII	IX	X	XI	XII
Ca^{2+}	R	2.40	2.46	2.52	2.58	2.63	—	2.74
	a	1021	996	972	950	932	—	894
	b	2.917	2.846	2.778	2.713	2.662	—	2.555
Sr^{2+}	R	2.58	2.61	2.66	2.71	2.76	—	2.84
	a	950	939	921	904	888	—	863
	b	2.713	2.682	2.632	2.583	2.536	—	2.465
Ba^{2+}	R	2.75	2.78	2.82	2.87	2.92	2.97	3.01
	a	891	881	869	854	839	825	814
	b	2.545	2.518	2.482	2.439	2.397	2.357	2.326

Table 5. Measured and calculated Raman and IR frequencies (in cm^{-1}) of the Γ-point phonons in La_2CuO_4. A prime denotes a displacement in the opposite direction (a 'counter-phase' vibration). O and O_{ap} stand for oxygens in the basal planes and apex oxygens, respectively. The symbols BB and BS denote bond-bending and bond-stretching.

Mode	Experiment			Calculation		Ionic disp.
	[44]	[45]	[48]	[48]	This work	
A_{1g}	226	228	228	180	220	La
A_{1g}	430	429	435	424	433	O_{ap}
E_g	—	—	—	106	104	La
E_g	—	230	—	297	233	O_{ap}
	[46]	[47]				
A_{2u}	240/—	242/—	234/342	213/229	220/257	Cu, La'
A_{2u}	—/463	342/—	354/466	349/411	337/463	Cu, O'
A_{2u}	501/574	501/—	516/576	509/509	486/500	O, O'_{ap}
B_{2u}	—	—	—	286	259	O
E_u	162/183	132/—	148/—	135/153	120/172	Cu, La'
E_u	220/250	—/—	—/290	168/252	175/241	Cu, O'_{ap}
E_u	363/390	358/—	359/446	359/448	366/440	Cu–O BB
E_u	671/683	667/—	669/694	662/685	655/668	Cu–O BS

The parameters of the shell model derived via fits to the measured values of ϵ_∞, c_{11} and c_{44}, and the experimental dispersion curves in three symmetry directions, are summarized in table 3. The calculated phonon curves are shown in figure 3 in comparison with the experimental points. For $\alpha^{(2)}$ a value of $2450\,\text{eV Å}$ was obtained.

Table 6. Measured and calculated Raman and IR frequencies (in cm^{-1}) of the Γ-point phonons in $YBa_2Cu_3O_6$. O and O_{ap} stand for planar and apex oxygens, respectively. Cu1 is a 'chain' copper ion and Cu2 is a planar one. The other notations are the same as in table 5.

Mode	Experiment		Calculation		Ionic disp.
	[51]	[52]	[50]	This work	
A_{2u}	107/109	105/110	116/119	109/116	Cu1, Cu2, Ba'
A_{2u}	154/180	146/180	153/163	140/185	Cu1', Cu2, Ba'
A_{2u}	217/220	215/222	189/203	185/290	Cu2, Ba, Y', O'
A_{2u}	442/458	367/470	390/455	367/422	Cu2, Y, O'
A_{2u}	648/663	645/664	540/543	621/671	Cu1, O'_{ap}
B_{2u}	—	—	—	190	O
E_u	—	—	55/62	81/82	Cu1, Cu2, Ba'
E_u	118/124	116/125	105/106	100/101	Cu1', Cu2, Ba'
E_u	190/195	188/199	214/243	178/193	Cu2, O, Y'
E_u	251/264	246/266	276/318	268/292	O_{ap}
E_u	361/418	351/420	355/414	351/423	Cu2–O BB
E_u	589/628	595/637	502/507	590/617	Cu2–O BS
	[53]		[50]	This work	
A_{1g}	115		121	113	Ba
A_{1g}	145		131	151	Cu2
A_{1g}	454		401	449	O
A_{1g}	472		484	470	O_{ap}
B_{1g}	341		352	320	O
E_g	—		—	60	Ba
E_g	—		—	149	Cu2
E_g	—		—	275	O_{ap}
E_g	—		—	387	Cu2–O BB
E_g	—		—	587	Cu2–O BS

The model parameters were applied in the lattice-dynamical study of Ca_2CuO_3, where each Ca ion is coordinated by seven oxygen ions, separated by different distances from it. The calculated phonon spectra of this compound were found to be stable and the eigenfrequencies to be in good correspondence with the experimentally measured ones [41]. This result can serve as evidence for the validity of the extrapolation scheme.

3.3. Rare earth cuprates

The parent compound La_2CuO_4 of the high-T_c superconducting family $(La, Sr)_2CuO_4$ is composed of a perovskite block $LaCuO_3$ and a rock-salt block LaO, sharing a common plane (figure 4). The copper ions in the perovskite block are octahedrically coordinated by four 'planar' oxygens O in the basal planes and by two, more distant, 'apex' ones O_{ap} along the c axis. The inelastic neutron diffraction measurements of pure La_2CuO_4 [42, 43] showed a behaviour typical for a 2d metal, because of the absence of LO–TO splitting of the E_u modes, polarized in the basal planes. This was not supported by the optical data [44–48], which indicated that this material is an insulator. All of the infrared active frequencies were observed, as well as the two A_{1g} Raman-active ones. The two remaining E_g modes are still not clearly positioned. The lower (lanthanum) E_g mode is expected to be situated below 100 cm^{-1} [42,43] and the higher (apex oxygen) one is probably near 230 cm^{-1} [45]. Bearing in mind that the interpretation of neutron scattering data for complex structures is not trivial and depends on additional assumptions, in the calculations described here only optical data were taken into account (see table 5).

Table 7. Measured and calculated Raman and IR frequencies (in cm^{-1}) of the Γ-point phonons in Nd$_2$CuO$_4$. O and O$_{xy}^z$ stand for planar oxygens and fluorite block oxygens, respectively. The other notations are as in table 5.

Mode	Experiment			Calculation		Ionic disp.
	[54]	[55]	[56]	[59]	This work	
A$_{1g}$	229	228	228	218	221	Nd
B$_{1g}$	330	333	328	328	320	O$_{xy}^z$
E$_g$	—	—	—	143	132	Nd
E$_g$	488	488	480	484	480	O$_{xy}^z$
A$_{2u}$		134/146	134/144	144/144	125/126	Cu, Nd'
A$_{2u}$		269/440	282/433	270/422	265/447	Cu, O', O$_{xy}^z$
A$_{2u}$		505/555	516/559	478/551	499/531	O, O$_{xy}^z$
B$_{2u}$		—	—	259	286	O
E$_u$		129/140	132/139	147/157	140/153	Cu, Nd'
E$_u$		300/342	304/341	317/331	316/346	Cu–O BB
E$_u$		350/437	353/432	344/424	363/450	Nd, O$_{xy}^{z'}$
E$_u$		509/595	512/593	490/590	513/594	Cu–O BS
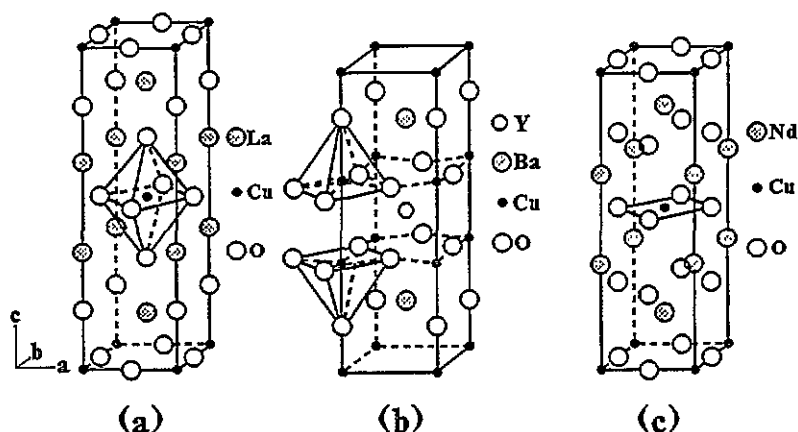
Figure 4. The unit cells of (a) La$_2$CuO$_4$, (b) YBa$_2$Cu$_3$O$_6$ and (c) Nd$_2$CuO$_4$.

The semiconducting tetragonal YBa$_2$Cu$_3$O$_6$, which is an oxygen-deficient analogue of the high-T_c superconducting compound YBa$_2$Cu$_3$O$_7$, is comprised of two types of oxygen-deficient perovskite blocks: ACuO$_{2.5}$ (where A = Y or Ba) and BaCuO (figure 4). In the ACuO$_{2.5}$ blocks copper is pyramidally coordinated by four planar oxygens O and an 'apex' oxygen O$_{ap}$. This compound was investigated both structurally [49] and optically [50–53] (see table 6). With the exception of the lowest (barium) E$_u$ mode, all the infrared active modes were reliably assigned. Among the Raman active modes, only those polarized along the c axis were observed in the Raman spectra.

Pure Nd$_2$CuO$_4$, which is the parent compound of the n-type high-T_c superconducting system (Nd, Ce)$_2$CuO$_4$, crystallizes in the T' phase (figure 4). This structure can be considered as consisting of oxygen-deficient perovskite blocks NdCuO$_2$ and fluorite blocks NdO. The copper ions are square coordinated by four planar oxygens and no 'apex' oxygens are present. Soon after the neodymium cuprate was synthesized, complete optical

Table 8. Short-range parameters for rare earth/yttrium–oxygen ionic pairs for N-fold cation coordination ($\alpha^{(3)} = 4000$ eV Å, $\beta = 7.00$.)

Ion	Parameter	Coordination number						
		VI	VII	VIII	IX	X	XI	XII
La^{3+}	R	2.432	2.5	2.56	2.616	2.67	—	2.76
	a	1645	1600	1563	1529	1498	—	1449
	b	2.878	2.800	2.734	2.676	2.622	—	2.536
Pr^{3+}	R	2.39	—	2.526	2.579	—	—	—
	a	1674	—	1584	1551	—	—	—
	b	2.929	—	2.771	2.714	—	—	—
Nd^{3+}	R	2.383	—	2.509	2.563	—	—	2.67
	a	1679	—	1594	1561	—	—	1498
	b	2.937	—	2.790	2.731	—	—	2.620
Sm^{3+}	R	2.358	2.42	2.479	2.532	—	—	2.64
	a	1696	1653	1614	1580	—	—	1515
	b	2.969	2.893	2.824	2.765	—	—	2.620
Eu^{3+}	R	2.347	2.41	2.466	2.52	—	—	—
	a	1704	1660	1622	1587	—	—	—
	b	2.983	2.905	2.839	2.778	—	—	—
Gd^{3+}	R	2.338	2.40	2.453	2.507	—	—	—
	a	1711	1667	1631	1596	—	—	—
	b	2.994	2.917	2.854	2.792	—	—	—
Tb^{3+}	R	2.323	2.38	2.44	2.495	—	—	—
	a	1722	1681	1639	1603	—	—	—
	b	3.013	2.941	2.869	2.806	—	—	—
Dy^{3+}	R	2.312	2.37	2.427	2.483	—	—	—
	a	1730	1688	1648	1611	—	—	—
	b	3.028	2.954	2.884	2.819	—	—	—
Ho^{3+}	R	2.301	—	2.415	2.472	2.52	—	—
	a	1738	—	1656	1618	1587	—	—
	b	3.042	—	2.899	2.832	2.778	—	—
Y^{3+}	R	2.300	2.360	2.419	2.475	—	—	—
	a	1739	1695	1654	1616	—	—	—
	b	3.043	2.966	2.894	2.828	—	—	—
Er^{3+}	R	2.29	2.345	2.404	2.462	—	—	—
	a	1747	1706	1664	1625	—	—	—
	b	3.057	2.985	2.912	2.843	—	—	—
Tm^{3+}	R	2.28	—	2.394	2.452	—	—	—
	a	1754	—	1671	1631	—	—	—
	b	3.070	—	2.924	2.855	—	—	—
Yb^{3+}	R	2.268	2.325	2.385	2.442	—	—	—
	a	1764	1720	1677	1638	—	—	—
	b	3.086	3.011	2.935	2.867	—	—	—
Lu^{3+}	R	2.261	—	2.377	2.432	—	—	—
	a	1769	—	1683	1645	—	—	—
	b	3.096	—	2.945	2.878	—	—	—

measurements were carried out [54–56] (table 7). The only 'problematic' mode is that of Nd with E_g symmetry, which was observed at 122 cm^{-1} [57] and at 126 cm^{-1} [58] as a

rather unclear feature in the Raman spectra.

The lattice dynamics of La_2CuO_4, $YBa_2Cu_3O_6$ and Nd_2CuO_4 were studied here using the assumptions listed in section 2, and the parameters of the rare earth/yttrium–oxygen SR interactions were supposed to obey the scaling laws (2.4) and (2.9). Such an assumption is acceptable because there is some freedom in the choice of the corresponding a and b parameters [14,60]. As input, Cu–O SR parameters, copper and oxygen shell charges and polarizabilities, the values for CuO, given in table 1, were adopted. The unknown parameters, including $\alpha^{(3)}$, were determined via fits to the measured optical frequencies (see tables 5, 6 and 7). The resulting values are $Y_{Re} = 1.7$, $\alpha_{Re} = 0.7\,\text{Å}^3$, $Y_Y = 2.0$, $\alpha_Y = 1.7\,\text{Å}^3$, $\alpha^{(3)} = 4000\,\text{eV Å}$. In order to get better correspondence with the observed A_{1g} and E_g modes in La_2CuO_4, following the proposition made in [48] the apex oxygen shell charge had to be reduced to -1.5 and its polarizability was considered anisotropic: along the c axis it was fixed at $2.0\,\text{Å}^3$ and in the ab plane it was fixed at $4.5\,\text{Å}^3$. In $YBa_2Cu_3O_6$ and Nd_2CuO_4 the polarizability of the planar oxygen ions along the c axis was raised to $3.0\,\text{Å}^3$ [10, 14]; the Cu–O_{ap} SR parameter b had to be additionally adjusted and its final values are $2.880\,\text{Å}$ (octahedra) and $3.444\,\text{Å}$ (pyramids). In the case of $YBa_2Cu_3O_6$ the ionic charge of the 'chain' copper was fixed at 1.0 and its SR interaction with the apex oxygens had to be diminished considerably: $b = 4.25\,\text{Å}^{-1}$. Finally, the shell charge of Ba was reduced to 3.0 in order to reproduce the two lowest (barium) A_{1g} and A_{2u} modes. The calculated phonon frequencies along with the corresponding ionic displacements are presented in tables 5, 6 and 7 in comparison with the measured modes. The a and b parameters for various rare earth/yttrium–oxygen ionic pairs are displayed in table 8 for different interionic separations R.

The model parameters proposed here were applied in the calculation of the phonon modes of $(Pr, Sr)_2CuO_4$ (T, T' and T^* phases) [61], $YBaCuFeO_5$ [62], $YBa_2Fe_3O_8$ [63] and $HgBa_2CuO_4$ [64]. The results obtained were successfully used in the assignment of the observed features in the measured optical spectra and for the prediction of the unobserved phonon modes.

In conclusion, a model approach to the lattice dynamics of layered copper oxides within a shell model has been presented. As well as implementing the idea of using parameters obtained from structurally similar substances, we implemented an extrapolation scheme for the derivation of the SR potential parameters for two groups of ionic pairs and for various cation coordinations. These parameters were applied in the dynamical calculations of several copper oxides, the results of which were found to be very helpful in the assignment of phonon modes.

Acknowledgments

References

[1]   Weber W 1987 *Phys. Rev. Lett.* **58** 1371
[2]   Brun T, Grimsditch M, Gray K E, Bhadra R, Maroni V and Loong C K 1987 *Phys. Rev.* B **35** 8837

[3] Stavola M, Krol D M, Weber W, Sunshine S A, Jayaraman A, Kouroulis G A, Cava R J and Rietman E A 1987 *Phys. Rev.* B 36 850
[4] Bates F E and Eldridge J E 1987 *Solid State Commun.* 64 1435
[5] Burns G, Dacol F H, Holtzberg F and Kaiser D L 1988 *Solid State Commun.* 66 217
[6] Bates F E 1989 *Phys. Rev.* B 39 322
[7] Brüesch P and Bührer W 1988 *Z. Phys.* B 70 70
[8] de Wette F W 1991 *Comment. Condens. Matter Phys.* 15 225
[9] Prade J, Kulkarni A D, F W de Wette, W Kress, M Cardona, R Reiger and U Schröder 1987 *Solid State Commun.* 64 1267
[10] Kress W, Schröder U, Prade J, Kulkarni A D and de Wette F W 1988 *Phys. Rev.* B 38 2906
[11] Prade J, Kulkarni A D, de Wette F W, Schröder U and Kress W 1989 *Phys. Rev.* B 39 2771
[12] Kulkarni A D, de Wette F W, Prade J, Schröder U and Kress W 1990 *Phys. Rev.* B 41 6409; 1991 *Phys. Rev.* 43 5451
[13] Humlíček J, Litvinchuk A P, Kress W, Lederle B, Thomsen C, Cardona M, Habermeier H-U, Trofimov I E and König W 1993 *Physica* C 206 345
[14] Rampf E, Schröder U, de Wette F W, Kulkarni A D and Kress W 1993 *Phys. Rev.* B 48 10143
[15] Allan N L and Mackrodt W C 1988 *Phil. Mag.* A 58 555; 1989 *Phil. Mag.* B 59 191
[16] Allan N L, Lawton J M and Mackrodt W C 1989 *J. Phys.: Condens. Matter* 1 2657
[17] Lewis G V and Catlow C R A 1985 *J. Phys. C: Solid State Phys.* 18 1149
[18] Pacchioni G, Sousa C, Illas F, Parmigiani F and Bagus P S 1993 *Phys. Rev.* B 48 11573
[19] Sharma J C, Shanker J and Goyal S C 1977 *J. Phys. Chem. Solids* 38 327
[20] Catlow C R A, Mackrodt W C, Norgett M J and Stoneham A M 1977 *Phil. Mag.* 35 177
[21] Singh R K and Singh S L 1982 *Phys. Status Solidi* b 112 717
[22] Born M and Huang K 1968 *Dynamical Theory of Crystal Lattices* (Oxford: Clarendon)
[23] Popov V N unpublished
[24] Shannon R D 1976 *Acta Crystallogr.* A 32 751
[25] Åsbrink S and Norrby L-J 1970 *Acta Crystallogr.* B 26 8
[26] Irwin J C, Chrzanowski J, Wei T, Lockwood D J and Wold A 1990 *Physica* C 166 456
[27] Reichardt W, Gompf F, Ain M and Wanklyn B M 1990 *Z. Phys.* 81 19
[28] Reichardt W, Wagner V and Kress W 1975 *J. Phys. C: Solid State Phys.* 8 3955
[29] Jacobson J L and Nixon E R 1968 *J. Phys. Chem. Solids* 29 967
[30] Pinchon G E and Sieckman M F 1966 *Phys. Rev.* 143 595
[31] Anderson C J and Hensley E B 1975 *J. Appl. Phys.* 46 443
[32] Dragoo A L and Spain I L 1977 *J. Phys. Chem. Solids* 38 705
[33] Son P R and Bartels R A 1972 *J. Phys. Chem. Solids* 33 819
[34] Vetter V H and Bartels R A 1973 *J. Phys. Chem. Solids* 34 1449
[35] Vijayaraghvan P R and Iyengar P K 1970 *Proc. Nucl. Phys. Solid State Phys.* 13C 439
[36] Saunderson D H and Peckham G 1971 *J. Phys. C: Solid State Phys.* 4 2009
[37] Rieder K H, Migoni R and Renker B 1975 *Phys. Rev.* B 12 3374
[38] Chang S S, Tompson C W, Gürmen E and Muhlestein L D 1975 *J. Phys. Chem. Solids* 36 769
[39] Singh R K 1982 *Phys. Rep.* 85 259
[40] Sangster M J L and Stoneham A M 1981 *Phil. Mag.* B 43 597
[41] Zlateva G A, Popov V N, Gyulmezov M, Bozukov L N and Iliev M N 1992 *J. Phys.: Condens. Matter* 4 8543
[42] Böni P, Axe J D, Shirane G, Birgeneau R J, Gabbe D R, Jenssen H P, Kastner M A, Peters C J, Picone P J and Thurston T R 1989 *Phys. Rev.* B 38 185
[43] Rietschel H, Pintschovius L and Reichardt W 1989 *Physica* C 162–4 1705
[44] Burns G, Chandrashekhar G V, Dacol F H and Shafer M W 1988 *Solid State Commun.* 68 67
[45] Weber W H, Peters C R and Logothetis E M 1989 *J. Opt. Soc. Am.* B 6 455
[46] Gervais F, Echegut P, Bassat J M and Odier P 1988 *Phys. Rev.* B 37 9364
[47] Collins R T, Schlesinger Z, Chandrashekhar G V and Shafer M W 1989 *Phys. Rev.* B 39 2251
[48] Mostoller M, Zhang J, Rao A M and Eklund P C 1990 *Phys. Rev.* B 41 6488
[49] Jogensen J D, Veal B W, Paulikas A P, Nowicki L J, Crabtree G W, Claus H and Kwok W K 1990 *Phys. Rev.* B 41 1863
[50] Thomsen C, Cardona M, Kress W, Lui R, Genzel L, Bauer M and Schonherr E 1988 *Solid State Commun.* 65 1139
[51] Crawford M K, Burns G and Holzberg F 1989 *Solid State Commun.* 70 557
[52] Bauer M, Ferreira I B, Genzel L, Cardona M, Murugaraj P and Maier J 1989 *Solid State Commun.* 72 551
[53] Heyen E T, Kircher J and Cardona M 1992 *Phys. Rev.* B 45 3037

[54] Hadjiev V G, Kostadinov I Z, Bozukov L, Dinolova E and Mateev D M 1989 *Solid State Commun.* **71** 1093

[55] Crawford M K, Burns G, Chandrashekhar G V, Dacol F H, Farneth W E, McCarron E M III and Smalley R J 1990 *Phys. Rev.* B **41** 8933

[56] Heyen E T, Kliche G, Kress W, König W, Cardona M, Rampf E, Prade J, Schröder U, Kulkarni A D, de Wette F W, Piñol S, McPaul D, Morán E and Alario-Franco M A 1990 *Solid State Commun.* **74** 1299

[57] Popovic Z V, Sacuto A and Balkanski M 1991 *Solid State Commun.* **78** 99

[58] Jandl S, Iliev M, Thomson C, Cardona M, Wanklyn B M and Chengkang C 1993 *Solid State Commun.* **87** 609

[59] Rampf E, Schröder U, de Wette F W, Kulkarni A D and Kress W 1993 *Phys. Rev.* B **48** 10143

[60] Popov V N and Valchinov V L 1990 *Physica* C **172** 260

[61] Mateev D M, Popov V N, Hadjiev V G and Iliev M N 1995 *Physica* C to be published

[62] Atanassova Y K, Popov V N, Bogachev G G, Iliev M N, Mitros C, Psycharis V and Pissas M 1993 *Phys. Rev.* B **47** 15201

[63] Atanassova Y K *et al* unpublished

[64] Popov V N and Hadjiev V G 1995 *Proc. 1994 NATO Advanced Study Institute on Fabrication, Properties and Application of Low-Dimensional Semiconductor Structures* ed M Balkanski (Dordrecht: Kluwer) to be published